Journal of Chromatography A, 1217 (2010) 225–234

Contents lists available at ScienceDirect

Journal of Chromatography A

journal homepage: www.elsevier.com/locate/chroma

Separation by hydrophobic interaction chromatography and structural determination by mass spectrometry of mannosylated glycoforms of a recombinant transferrin-exendin-4 fusion protein from yeast

Melissa D. Zolodz[a,1], John T. Herberg[b,1], Halyna E. Narepekha[a], Emily Raleigh[b], Matthew R. Farber[a], Robert L. Dufield[a], Denis M. Boyle[b,*]

[a] Analytical Research and Development, Pfizer Global Biologics, Chesterfield, MO 63017, USA
[b] Bioprocess Research and Development, Pfizer Global Biologics, Chesterfield, MO 63017, USA

ARTICLE INFO

Article history:
Available online 30 October 2009

Keywords:
Hydrophobic interaction chromatography (HIC)
Mannosylation
Transferrin
Yeast
Mass spectrometry
ETD
NPLC/MS

ABSTRACT

Obtaining sufficient amounts of pure glycoprotein variants to characterize their structures is an important goal in both functional biology and the biotechnology industry. We have developed preparative HIC conditions that resolve glycoform variants on the basis of overall carbohydrate content for a recombinant transferrin-exendin-4 fusion protein. The fusion protein was expressed from the yeast *Saccharomyces cerevisiae* from high density fermentation and is post-translationally modified with mannose sugars through O-glycosidic linkages. Overall hydrophobic behavior appeared to be dominated by the N-terminal 39 amino acids from the exendin-4 and linker peptide sequences as compared to the less hydrophobic behavior of human transferrin alone. In addition, using LC techniques that measure total glycans released from the pure protein combined with new high resolution technologies using mass spectrometry, we have determined the locations and chain lengths of mannose residues on specific peptides derived from tryptic maps of the transferrin-exendin-4 protein. Though the protein is large (80,488 kDa) and contains 78 possible serine and threonine residues as potential sites for sugar addition, mannosylation was observed on only two tryptic peptides located within the first 55 amino acids of the N-terminus. These glycopeptides were highly heterogeneous and contained between 1 and 10 mannose residues scattered among the various serine and threonine sites which were identified by electron transfer dissociation mass spectrometry. Glycan sequences from 1 to 6 linear mannose residues were detected, but mannose chain lengths of 3 or 4 were more common and formed 80% of the total oligosaccharides. This work introduces new technological capabilities for the purification and characterization of glycosylated variants of therapeutic recombinant proteins.

1. Introduction

Hydrophobic interaction chromatography (HIC) is widely used in the purification of proteins. HIC exploits the binding between hydrophobic patches on the surface of proteins and a nonpolar ligand immobilized to a solid support [1,2]. The main factors affecting protein retention to a hydrophobic support are the type and concentration of salt used [3,4], and the hydrophobicity and density of the immobilized ligand [5,6]. Temperature, pH and other conditions employed during binding such as chromatographic flow rate can also exert major effects. In classical HIC, protein binding is typically achieved by high salt concentrations that specifically promote these interactions, while desorption is controlled either by isocratic elution or by gradual removal of these salts from chromatography columns [7]. Other components, often nonpolar but water soluble additives can also be used to control elution selectivity [8,9]. The complex selectivity behavior of proteins on HIC media has been estimated from intrinsic protein properties relating to their hydrophobic surface properties [4,10], and has been proposed as resulting from specific structural changes, i.e., spreading or unfolding of the protein during adsorption [11], the distribution of salt ions and water molecules during binding [12], or by different preferred binding orientations of the protein or a combination of different mixed mode interactions [13,14].

The usefulness of HIC for the purification of proteins comes from an ability to separate closely related variants by varying chromatographic selectivity through mobile phase changes while still retaining high adsorptive capacities for preparative purposes. Fur-

* Corresponding author at: Pfizer Inc., BB3D, 700 Chesterfield Village Parkway West, Chesterfield, MO 63017, USA. Tel.: +1 636 247 6394; fax: +1 636 247 6511.
E-mail address: denis.m.boyle@pfizer.com (D.M. Boyle).
[1] These authors contributed equally to this work.

0021-9673/$ – see front matter © 2009 Elsevier B.V. All rights reserved.
doi:10.1016/j.chroma.2009.10.057

thermore, requirements in the biotechnology industry demand uniformly high purity preparations with a high degree of structural knowledge of the components, which in turn require highly resolving and scaleable technologies along with the analytical tools to produce them. The large scale synthesis of heterologous proteins from recombinant systems nearly always results in small amounts of structural heterogeneities of the desired protein as part of the complex mixture [15,16]. These arise during translation or result from chemical modifications incurred during purification (post-translational modifications, sequence variations generated from proteolysis or transcriptional/translational errors, and degradation products) [17], and are important because any of these can potentially affect the target activity profile of a proposed therapeutic protein. Variants at the primary sequence level such as truncations or mis-incorporations [18,19], oxidations/deamidation [20] and glycosylation [21,22] variants, or multimeric aggregated impurities [23] frequently have altered charge properties to allow separation of species by traditional ion exchange methods, but this is not always the case. The use of HIC in preparative mode to separate uncharged protein variants from the primary target species, such as glycoprotein isoforms in semi-purified preparations, is especially appropriate.

Control of protein glycosylation patterns in particular is an important consideration for the choice of expression system for biotechnology products. The glycosylation pattern of circulating proteins or peptides significantly affects their fate *in vivo*, such as their resistance to proteolysis [24] (including transferrin [25]), effects upon plasma half-life [26], immunogenicity [27–29] or bioactivity [30–32]. Both the total amount and specific type of glycan structures attached to the parent molecule must be evaluated during manufacturing to maintain a consistent pharmacokinetic profile and avoid undesirable side effects. Human glycoproteins have both N- and O-linked glycan structures and most marketed recombinant proteins are currently produced from mammalian cell platforms [33]. Heterologous proteins produced from yeast also contain both N- and O-linked glycoproteins, and typically O-linked glycoproteins are produced as long linear chains of mannose [2,34]. For example, transferrin has been produced from both *Pichia pastoris* [35–37] and *Saccharomyces cerevisiae* [38]; this is consistent with the use of these systems to produce several protein biotherapeutic candidates [33]. Other key benefits include the development of yeast strains that can be efficiently and stably transformed with foreign genes, secrete large amounts of protein, and show vigorous growth at high density with straightforward scale-up on inexpensive substrates.

In this paper, we used HIC to separate glycosylated isoforms (mannosylated glycoproteins) of a purified recombinant transferrin-exendin-4 fusion protein (Tf-exendin) produced in the yeast *S. cerevisiae*. The extent of glycosylation is not predictable in yeast proteins and they are usually produced as complex mixtures [34]. Addition of the first mannose residue on serine and threonine residues occurs in the ER, while linear elongation of mannose residues through mannosyltransferase enzymes occurs in the Golgi [21,39]. Also presented are new mass spectrometric glycan analysis methods to characterize the mannosylated glycoprotein variants. Due to its complex degree of modification, several new technologies were optimized to characterize the extent of this heterogeneous post-translational modification. Recombinant proteins grown in yeast provide a unique set of analytical challenges but are viable candidates for characterization utilizing mass spectrometry such as linear ion trap mass spectrometry. We first coupled traditional glycan normal phase HPLC (NPLC) to ESI mass spectrometry to determine glycan length. Since O-linked glycosylations sites are not constricted to any consensus site sequence, determining the location of the oligosaccharides and elucidating site occupancy can be a cumbersome and difficult task [34]. A key technology in the present work is the dual use of Collision Induced Dissociation (CID) and Electron Transfer Dissociation (ETD) [40,41]. With CID, the weakest bonds break first (such as labile glycosylation bonds) which prevents determining the site of glycosylation [42]. However, with ETD, an electron from an electron donor anion (such as fluoranthene) produces charged peptide ions and fragmentation occurs along the peptide backbone almost randomly [43]. ETD is a particularly effective tool to locate the sites of glycosylation. The oligosaccharide remains attached to the serine/threonine residues providing ions with both the peptide sequence, the site of the glycan and the length of the glycan. We can use the property of neutral loss of the sugar via CID to locate the glycopeptides in the tryptic peptide map to trigger this ETD process. This method is termed "neutral loss-dependent ETD" (NL-dependent ETD) and is a form of tandem mass spectrometry used in LC/MS peptide mapping experiments to determine peptide sequence, glycosylation site and glycan size on each amino acid [44]. Tandem LC/MS via neutral loss of sugar moiety with CID followed by ETD on the precursor ion was optimized to locate glycosylation sites. The linear ion trap (LIT) mass spectrometer with its dual fragmentation methodologies is a particularly valuable tool in the characterization of recombinant yeast proteins. These data were used to provide structural assignments for both the length and location of mannose residues to relate these structural characteristics to their observed behavior in HIC.

2. Materials and methods

2.1. Preparation of purified transferrin fusion protein

The 80,488 kDa fusion protein consists of exendin-4, a 39 amino acid GLP-1 peptide agonist [45] at the N-terminus, then a 12 amino acid linker sequence (PEAPTDPEAPTD) from human transferrin followed by the complete sequence of 679 residues for transferrin. Two N-linked glycosylation sites (S466A, T664A) in the molecule have been eliminated, but there are 78 serine and threonine residues as possible O-linked glycosylation sites. Recombinant human transferrin (hTf) purified from *S. cerevisiae* without N-linked sites was used as a control in the studies. Briefly, protein was purified as a secreted protein from broth obtained from 11 L of high density, fed-batch fermentation broth of *S. cerevisiae*. Soluble Tf-exendin protein (1.8 g protein/L cell-free supernatant solution) was collected following removal of cells by a continuous operation using centrifugation, re-centrifugation of resuspended solids, microfiltration through a 1000 K molecular weight cut off (MWCO) membrane followed by retention and concentration by ultrafiltration using a 30 K MWCO membrane. Purification was accomplished as follows: SO_3 fractogel chromatography, α-mannosidase (Jack bean) digestion of the product pool for 24 h. at pH 5.0 and enzyme: protein ratio of 25.5:1 (w/w) in 1 mM $ZnSO_4$, Butyl Sepharose-HP chromatography, ultrafiltration/diafiltration (50 K MWCO), Poros 50HQ chromatography followed by a final ultrafiltration/diafiltration. Purified protein was stored frozen at 20 mg/mL in buffer consisting of 20 mM L-histidine, 20 mM sodium phosphate, 90 g/L trehalose, 0.1 g/L L-methionine, pH 7.3.

2.2. Hydrophobic interaction chromatography (HIC) conditions

All chemicals used for the preparation of buffers were USP grade and were obtained from VWR Scientific (Westchester, PA, USA). Buffers were prepared and pH adjusted at room temperature (18–22 °C). Butyl Sepharose-HP resin was obtained from GE Healthcare (Piscataway, NJ, USA) and Toyopearl Butyl 650S was obtained from Tosoh Bioscience (Montgomeryville, PA, USA). Chromatography experiments were performed at room temperature by using a GE Healthcare AKTA Explorer 100 automated chromatography

station. Tricorn columns (0.5 cm i.d. × 20 cm or 1.6 cm i.d. × 20 cm) were obtained from GE Healthcare and packed per the manufacturers recommendations. The column was equilibrated immediately prior to sample application with five column volumes (CV) of Buffer A (0.03 M Na HEPES 0.7 M Na_2SO_4, pH 7.5) at a flow rate of 70 cm/h. All subsequent column operations were performed at 150 cm/h except cleaning in 0.5 M NaOH which was performed at 60 cm/h. After sample application, the column was washed with five column volumes of Buffer A and then eluted with a 20 column volume (CV) gradient to 100% Buffer B (0.03 M Na HEPES, pH 7.5). Protein was loaded onto columns at approximately 5 mg protein/mL resin though up to 10 mg/mL was possible without yield losses. Detection was performed with online UV and conductivity meters and 0.5 CV fractions were collected.

2.3. Urea reversed phase HPLC (RP-HPLC) separation of glycoforms

HIC fractions were analyzed for relative levels of mannosylated species using RP-HPLC on an Agilent system (model 1100 and 1200) equipped with diode array or variable wavelength detector, a quaternary or binary pump, and a Zorbax 300SB-C_{18} column (3.5 μm, 4.6 mm × 150 mm) heated to 50 °C. The equilibration mobile phase and elution mobile phase both used a stock solution of deionized 8 M urea solution for their preparation. The urea was deionized by mixing BioRad AG 501-X8 (D) resin and for approximately 15–20 min or until the conductivity was <10 μS/cm. Prior to analysis, protein samples were centrifuged at 5000 rpm for 5 min. An aliquot of the supernatant was removed and 15 μg of protein was loaded onto the column. If a dilution was required, Milli-Q was utilized. Otherwise the injection volume was adjusted to achieve the targeted protein load. The equilibration mobile phase A was 0.1% TFA, 8 M urea and the elution mobile phase B was 0.1% TFA, 4 M urea in 50% acetonitrile. Using a flow rate of 0.5 mL/min, the column is equilibrated for 2 min at 60% B immediately before injection of protein followed by gradient elution from 60% to 79% B between 2 and 25 min and detection of Tf-exendin proteins at 230 nm. The column is then regenerated at 95% B for 1 min (79–95% in 0.1 min) followed by re-equilibration for 8.8 min (95–60% in 0.1 min) prior to the next injection. The column was stored in 50% Milli-Q purified water, 50% acetonitrile solution after use.

2.4. LC/MS of intact protein

Intact protein mass spectrometry analysis was performed via RP LC/MS using an Agilent 1100 HPLC equipped with diode array coupled to a Waters Micromass QTOF mass spectrometer. 15 μg was injected on an Agilent Zorbax 300SB-C_{18} column (3.5 μm, 4.6 mm × 150 mm) heated to 50 °C. The method was identical to the urea RP-HPLC method described above but without urea in the mobile phase. The flow rate was 0.5 mL/min and was split 50:50 prior to entering the source of the mass spectrometer. The ESI-QTOF was operated under collisional cooling conditions to focus the ion beam into the mass spectrometer [46]. The spray voltage was set to 3.0 kV and the cone voltage was operated at 80 V. The rf only quadrupole pressure was increased to 4.5 mTorr (as measured by the backing Pirani gauge). Data were collected at an m/z range of 1500–3500. ESI spectra were deconvoluted to zero charge spectra using MaxEnt software.

2.5. Analysis of released glycans by normal phase HPLC (NPLC) with fluorescent and mass spectral detection

O-linked glycans were released from the glycoprotein by ammonia-based, non-reductive β-elimination reaction [47]. Samples were diluted to 1 mg and desalted with Nanosep (Pall Life Sciences) membrane filters (MWCO 10 K). Desalted glycoprotein was dissolved in 1 mL of 28% aqueous ammonium hydroxide solution (Sigma–Aldrich, St. Louis, MO), saturated with ammonium carbonate (Sigma–Aldrich, St. Louis, MO), in a 1.5 mL Eppendorf microtube. An additional 100 mg of ammonium carbonate solid was added to the reaction mixture and incubated at 60 °C for 40 h. Salt was removed by repeated evaporation of water using speed-vac until no salt was noticeable in the micro tube. Ten microliters of 0.5 M boric acid (Sigma–Aldrich, St. Louis, MO) was added to the mixture and incubated at 37 °C for 30 min. Boric acid was removed by evaporation under nitrogen with several additions of methanol. Finally, the dried sample was dissolved in 50 μL of water and centrifuged. The insoluble peptides were discarded and supernatant containing glycans was used for fluorescent labeling in the next step. Solvent was removed from glycan samples via speed-vac prior to the labeling reaction. Glycans were then labeled with 2-aminobenzamide (2-AB) (Prozyme, San Leandro, CA) at 65 °C for 4 h. Excess labeling reagent was removed using a GlycoClean S cartridge (Prozyme, San Leandro, CA). Finally, the mixture of labeled glycans was analyzed by NPLC on an Agilent 1100 liquid chromatograph (Agilent Technologies, Palo Alto, CA) equipped with a fluorescence detector. The excitation wavelength was 330 nm and the emission wavelength was 420 nm. A GlycoSep™ N column (250 mm × 4.6 mm, 5 μm silica) held at 30 °C was used for the separation (Prozyme, San Leandro, CA). A gradient separation was used at a flow rate of 0.4 mL/min, starting with 80% A and 20% B and increasing to 53% B over 132 min. Mobile phase B was then increased to 100% over 3 min, held for 7 min and then down to 20% for re-equilibration. The mobile phases used were as follows: mobile phase A was acetonitrile and mobile phase B was 50 mM ammonium formate pH 4.4. An injection volume of 10 μL was used for HPLC analysis. In addition, 1 mM sodium acetate (Sigma–Aldrich, St. Louis, MO) added to mobile phase B to aid in sugar ionization. For NPLC/MS analyses, the column eluent was split 50:50 post-fluorescent detector and coupled to a ThermoScientific LTQ XL electrospray linear ion trap mass spectrometer. The mass spectrometer ESI voltage was operated at 5.5 kV, capillary voltage at 40 V, tube lens at 180 V, capillary temp set to 350 °C, and sheath gas flow was set to 30.

2.6. Glycopeptide analysis by LC/MS and LC/neutral loss-dependent electron transfer dissociation MS/MS (LC/NL-ETD MS/MS)

Samples were digested with trypsin (Promega, Madison, WI) at a 1:20 enzyme to substrate ratio in 26% acetonitrile (ACN), 26 mM Tris, pH 7.0 at 37 °C overnight. Digestion was quenched with 25 μL 0.1% TFA. Acetonitrile was removed via speed-vac for 20 min at RT. LC/MS and LC/NL-dependent ETD MS/MS analyses were performed by using an Agilent 1200 HPLC equipped with a C_{18} 2.1 mm × 150 mm RP Low TFA MS (Grace Vydac) column coupled to a ThermoFischer Scientific LTQ XL electrospray linear ion trap mass spectrometer with electron transfer dissociation capabilities. The digest mixture was diluted 1:1 with water and 40 μg was injected onto the column. Mobile phase A was composed of 0.01% TFA in water and mobile phase B contained 0.01% TFA in acetonitrile. The flow rate was 0.2 mL/min and the column was equilibrated at 95% A and was held for 5 min after injection. The gradient was adjusted linearly to 30% A over 85 min and then held for 5 min. The mobile phase was then returned to 95% A over 1 min followed by 15 min at 95% A for re-equilibration. The HPLC UV detector was a photodiode array. The ESI voltage was operated at 5.3 kV, capillary voltage 35 V, tube lens 50 V, capillary temp 370 °C, and sheath gas flow was set to 15. ETD conditions included nitrogen as the CI gas, fluoranthene as the electron donor, and the reaction time was set to 150 ms with supplemental activation for +2 charge state ions.

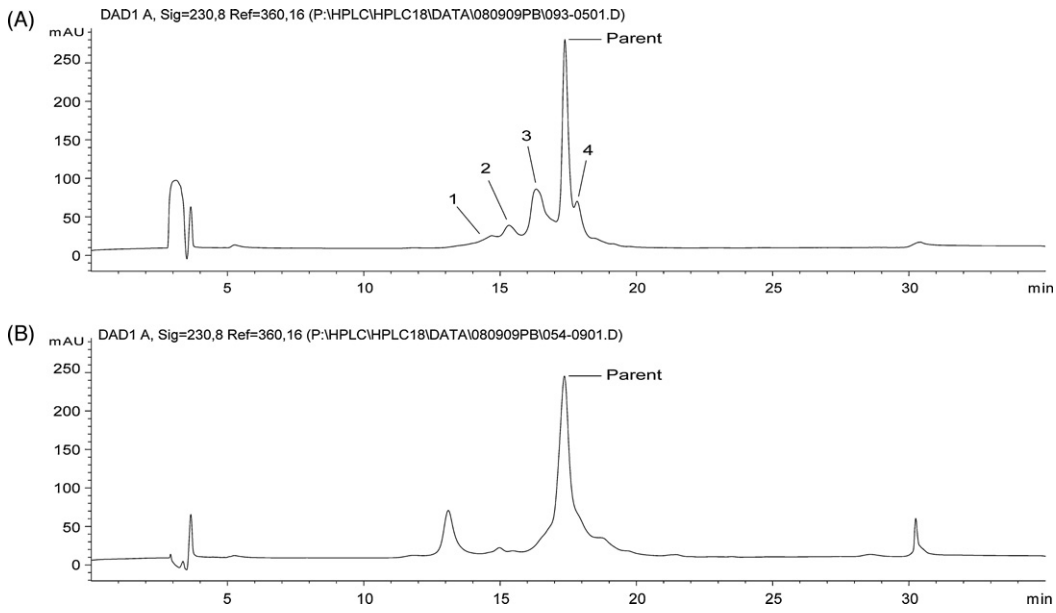

Fig. 1. (A) Urea RP-HPLC profile of purified Tf-exendin fusion protein showing structural heterogeneity due to early eluting, hydrophillic mannosylated glycoforms (peaks 1–3 identified by arrows). The parent peak (≤1 mannose/protein) is shown as the main component eluting at R_t = 17.5 min shown with a later eluting shoulder peak (peak 4) identified as carbamylated (+43 Da) Tf-exendin protein. (B) Urea RP-HPLC profile of purified Tf-exendin fusion protein treated with α-mannosidase during purification. The de-mannosylated Tf-exendin sample is lacking peaks 1–3 that elute at the same retention time as the Tf-exendin mannosylated glycoforms, but also contains a peak that that carried through purification that has the same retention time (R_t = 13.2 min) of a Tf-exendin variant truncated between amino acid residues 45 and 46 (D, P) as a result of low pH conditions required for the enzymatic digestion.

The scan sequence was devised to perform full scan, CID, and trigger ETD on the precursor ion but only when a neutral sugar loss occurred, i.e., "NL-dependent ETD". Five CID scans were repeated (top 5) and if no NL of 162 Da was observed the scan sequence was repeated starting with a full scan. Peptide sequence and mannosylation assignments were performed using BioWorks software (ThermoFischer Scientific, Waltham, MA) and *de novo* sequencing.

3. Results and discussion

The chromatographic separation of glycoproteins on the basis of small variations in carbohydrate composition is especially challenging when the glycan structures are uncharged or there are only subtle differences between attached sugars. Differences in sugar type and chain length, the presence of possible branched structures and their point of attachment at multiple sites along the length of the protein complicate the task further. Comparatively, the Tf-exendin protein with the N-linked sites removed is a less complex glycoprotein since it contains only linear mannose residues at serine and threonine residues. This makes it a good experimental choice to probe the role of sugar in the interactions between the protein backbone and hydrophobic ligand on a chromatographic support. In addition, a main goal of the present work was to produce preparations of pure protein at high yields with the least amount of mannose content for further commercial evaluation.

The first indication of the extent of variably mannosylated species present in purified samples of Tf-exendin protein was observed by urea RP-HPLC analysis. As shown in Fig. 1, several peaks are observed (peaks 1–4) within a small elution window between 14 and 18 min. These results suggest that these species are similar to one another structurally, but differed on the basis of polar modifications such as sugar content since SDS-PAGE results indicated a pure protein preparation (data not shown). The sharp main peak in Fig. 1 that elutes at R_t = 17.5 min indicates this species (52.5% by area) may be the most homogeneous component of the mixture and contained the least amount of mannose modifications. The broader peaks preceding main parent peak were less resolved from each other suggesting multiple species with higher mannose content. This result also suggested that differences in hydrophobicity could be exploited on a preparative scale to resolve variably mannosylated forms of the protein.

From initial screening results using short chain HIC resins containing an ether, methyl or Butyl-FF ligand (resins from Tosoh Co., BioRad Co. and GE Healthcare, respectively) and a 1–0 M ammonium sulfate system, a correlation between hydrophobicity and protein adsorption was established resulting in the selection of specific Butyl ligand chromatographic supports. From these data, even when protein was bound to weaker hydrophobic resins, little resolution of the components was possible. A small bead size (average 35 μm) was shown to be important for maximal resolution of Tf-exendin glycoforms [48]. The chromatograms in Fig. 2 compare performance using two different chromatographic resins, Butyl-HP shown in Fig. 2A with urea RP-HPLC results of the column fractions for this column in Fig. 2B, and Butyl 650S shown in Fig. 2C along with RP results of column fractions for this column in Fig. 2D. These profiles were obtained at 5 mg/mL resin protein loadings, a 4 mL column bed volume scale and were eluted with a reverse salt gradient from 700 mM to 0 mM sodium sulfate in buffer. Each of the Butyl columns runs produced similar results, i.e., three main peaks with poor resolution. However, the RP results indicated a better separation of mannosylated peaks 1–3 was obtained from the main parent peak (including nearly complete resolution of peaks 1 and 2 from parent) than is apparent from observation of the UV trace alone. Also shown for reference in Fig. 2B and D is the UV trace (solid line) from each column run overlaid with the RP results for the fractions. Using the RP data of the fractions, pools to enrich parent peak were made which excluded any fraction that was <80% parent by urea RP-HPLC area percent up to the valley of the last small peak within the gradient and excluded fractions thereafter. This produced a product pool for the Butyl-HP column of 78.2% main parent peak (includes some peak 4) purity and a column yield of 58.5%. Similarly, for the Butyl 650S column, a product pool of 75.8% main parent peak purity and a column yield of 55.9% were obtained. Thus, reproducible HIC column conditions were established with

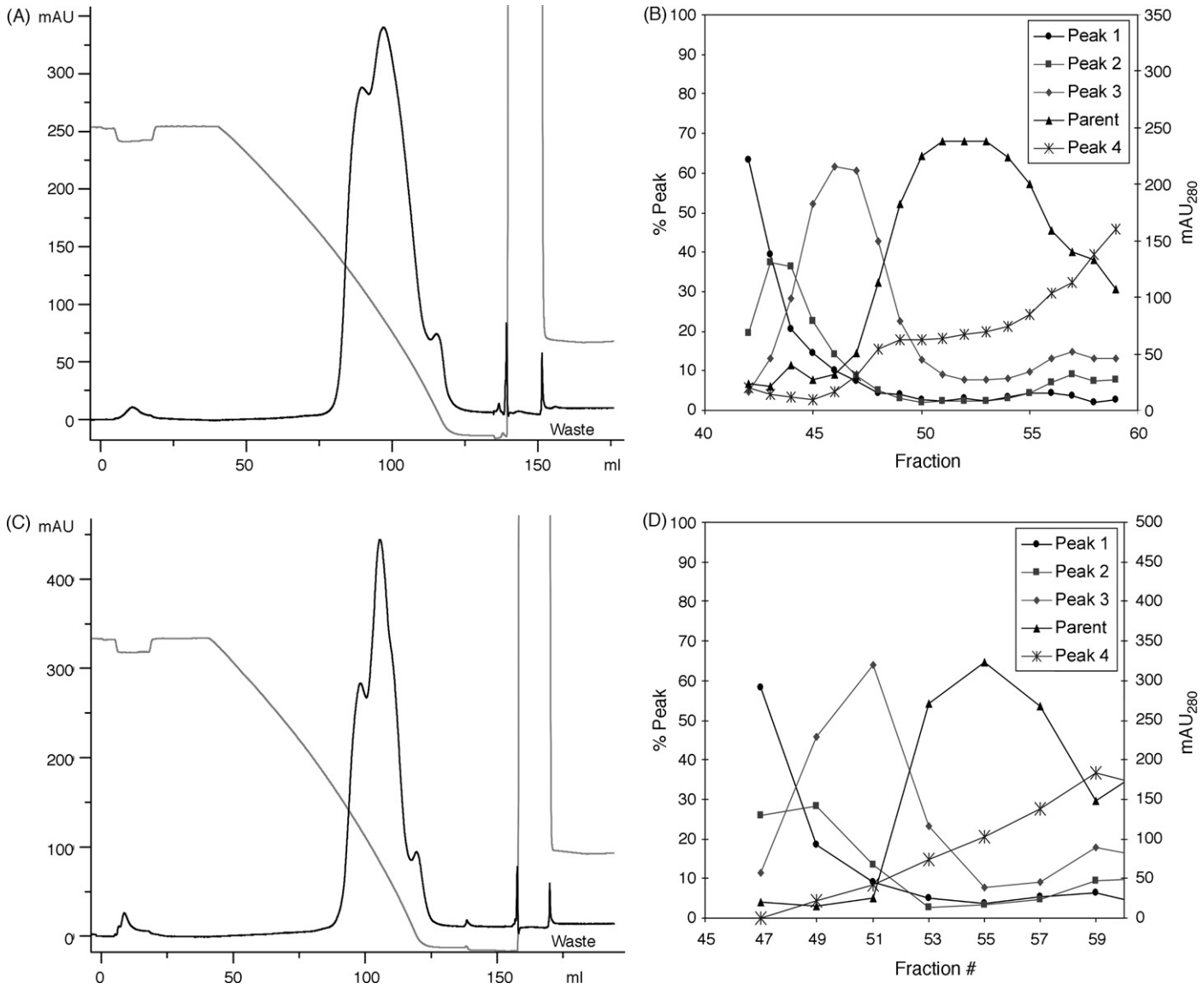

Fig. 2. UV chromatograms (λ = 280 nm) demonstrating the resolution of Tf-exendin fusion glycoforms by Butyl HIC with fraction analysis by urea RP-HPLC. Tf-exendin protein was adsorbed (5 mg/mL resin) onto a 4 mL bed volume column and eluted with a 20 CV reverse salt gradient of sodium sulfate (700–0 mM) in 30 mM HEPES, pH 7.5 from: (a) Butyl-HP or (c) Butyl 650S resins. In addition, 0.5 CV fractions were collected and analyzed by urea RP-HPLC within 24 h for (b) Butyl-HP and (d) Butyl 650S column runs.

reasonable yields that significantly improved main parent peak purity for two different chromatographic supports that could be adapted to pilot scale. All subsequent development and scale-up runs were performed using the Butyl-HP resin. Previous attempts to resolve glycoproteins have focused on the separation of sialylated glycoforms and have typically involved charged methods such as chromatofocusing [49], isoeletric focusing [50] or anion exchange [51] (the latter two references apply to human serum transferrin glycoforms). The separation of different sialylated glycoproteins by HIC has also been reported [52], but the present work appears to be the first demonstration of the preparative resolution by HIC of such closely related neutral mannosylated glycoforms.

To study the role mannosylation played on the behavior of Tf-exendin variants on HIC required additional structural information. First, recombinant human Tf protein grown in yeast similarly containing only O-linked sites was analyzed by urea RP-HPLC to compare to Tf-exendin, which contains an additional N-terminal exendin and linker sequence. Human Tf elutes significantly earlier than Tf-exendin protein suggesting that the significantly greater hydrophobic character of Tf-exendin is derived from the exendin and linker sequences. Human Tf has only one less O-linked glycosylation site than Tf-exendin (Fig. 3) within the first 55 amino acids of the N-terminus (8 vs. 9), and assuming an equal potential for mannosylation during protein synthesis for each molecule, human Tf could be hyper-mannosylated compared to Tf-exendin to account for its greater hydrophilicity during RP-HPLC. Human Tf is very hydrophilic and highly soluble in water (>90 mg/mL) and normally assumes a compact shape [53]. Also shown is the RP trace for Tf-exendin that was enzymatically de-mannosylated but which retains the exendin and linker sequences. Not only are peaks 1–3 absent when the sugars are removed (directly demonstrating their identity as mannosylated variants) but the elution position of the main peak parent is unchanged, as expected. The main parent peak likely had little mannose to begin with, but if the removal of all mannose residues from Tf-exendin did not affect intrinsic protein hydrophobicity of parent during RP-HPLC, then the exendin and linker sequence are in fact exerting a disproportionately large effect upon binding. This result also demonstrates that the addition of polar molecules such as sugars affected hydrophobic selectivity for the complete Tf-exendin molecule at the site of

Fig. 3. Comparison of first 55 amino acids from the N-terminus for both human transferrin (hTf) and Tf-exendin fusion protein showing number and location of serine and threonine residues as potential O-glycosylation sites: a total of 8 in hTf and 9 in Tf exendin. Linker sequence in Tf-exendin is PEAPTDPEAPTD. The cleavage sites and complete sequences for the first four tryptic peptides of Tf-exendin protein are indicated by vertical dashed lines and are labeled T1–T4. Note that only T1 and T4 contain potential O-linked sites. Hydrophobic amino acids F, L, M, V, W, I, A and P are italicized.

protein–ligand binding within this short sequence of 55 amino acids. Each of these two proteins has a total of 23 hydrophobic amino acids in the same segment (Fig. 3, italicized) yet exhibit very different elution behavior on urea RP-HPLC. This difference in selectivity is not fully understood; it may explained by a generally more solvent accessible N-terminus for peptides added to hTf, or the condition and solvents from RP chromatography may be promoting a different interaction than observed during true Butyl HIC with water and salt. A more specific explanation may be that enhanced adsorption from the hydrophobic amino acid sequence(s) in the unmannosylated T2 and T3 peptides in Tf-exendin are controlling hydrophobic selectivity; no similar serine/threonine-free stretch of 20 amino acids is present in the same sequence for hTf. Therefore a comparison of the total mannose content with structural configuration details for both molecules would also be useful to determine how these particular structural characteristics influence intrinsic exendin/linker hydrophobicity and the observed interactions of Tf-exendin with immobilized hydrophobic ligands. It would also be interesting to see how well human Tf glycoform variants from yeast can be resolved from each other in this system.

Additional results demonstrating the direct role that elevated mannose content plays in the elution of Tf-exendin peaks 1–3 were observed during LC/MS analysis. Using LC/MS analysis, highly mannosylated protein was separated by LC/MS using the chromatography shown in Fig. 1 but without urea to allow for ionization. The Tf-exendin protein resolved into several peaks via LC/MS and multiple additions of 162 Da indicative of a hexose were observed. Monosaccharide analysis via high pH anion exchange chromatography with pulsed amperometry detection indicated that mannose was the only sugar present (data not shown). Therefore, it is reasonable that the 162 Da additions correspond to mannose moieties. The intact protein was observed to be mannosylated up to seven times in peak 1/2. It is possible that variants of the protein contain more than seven mannose groups, but these polar molecules have a suppression effect on ionization. As a result, as the number of mannose residues increase the signal intensity or signal to noise ratio can decrease. Furthermore zero to five mannose moieties per protein were observed in peak 3. The fourth peak contained the unmodified parent protein, endogenously carbamylated protein and one putative mannose group [44]. Material that did not bind to a Concanavilin A column was also shown to be consistent with parent peak by LC/MS (data not shown).

Next, we determined the mannose chain length and their relative abundance on Tf-exendin. Glycans were released from protein

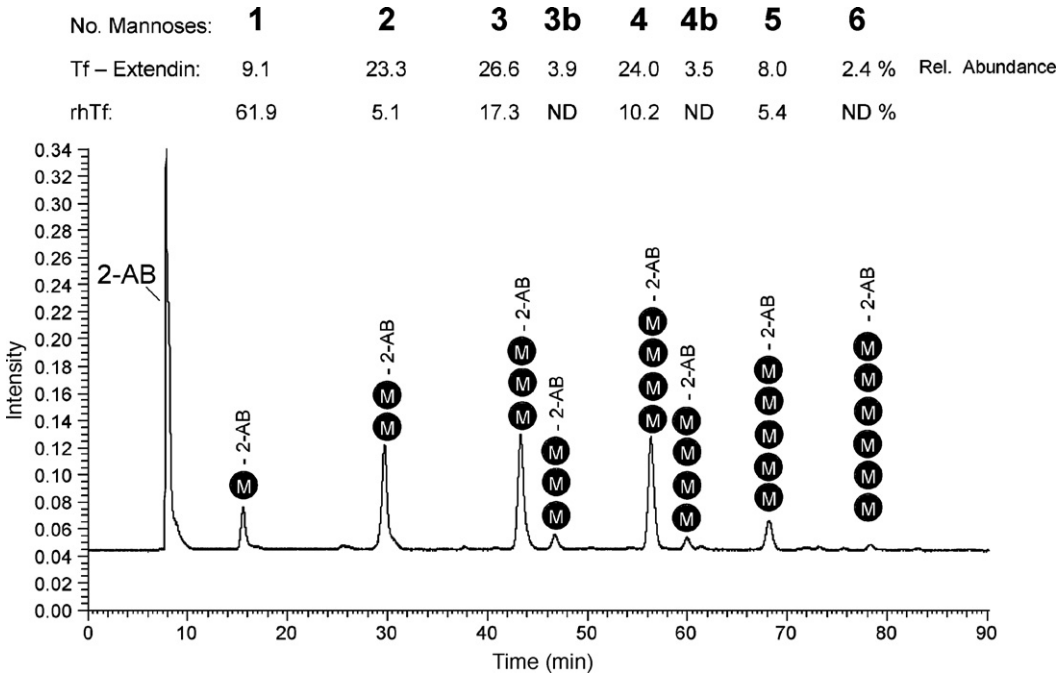

Fig. 4. Summary of NPLC/MS analysis of released O-linked glycans from Tf-exendin and recombinant human Tf (rhTf). The fluorescence trace of 2-AB labeled O-linked glycans released from Tf-exendin fusion protein is displayed. Samples were prepared as described in the methods section. Mannose glycans were observed as sodiated peaks $(M+Na)^+$ in the LTQ mass spectrometer. Up to 6 mannose moieties (hexamannose) were observed as released glycans from the Tf protein. Peaks 3 and 3b as well as 4 and 4b are resolved by NPLC and have the same number of residues (same molecular weights) which indicate different mannose linkages. The numbers above the fluorescence trace refer to mannose chain length. Below, the relative abundance of each glycan (calculated from fluorescent peak areas) from Tf-exendin is compared with those for recombinant hTf. Total carbohydrate content of recombinant hTf was approximately 26% of the entire sugar content from Tf-exendin fusion protein. ND: not detected.

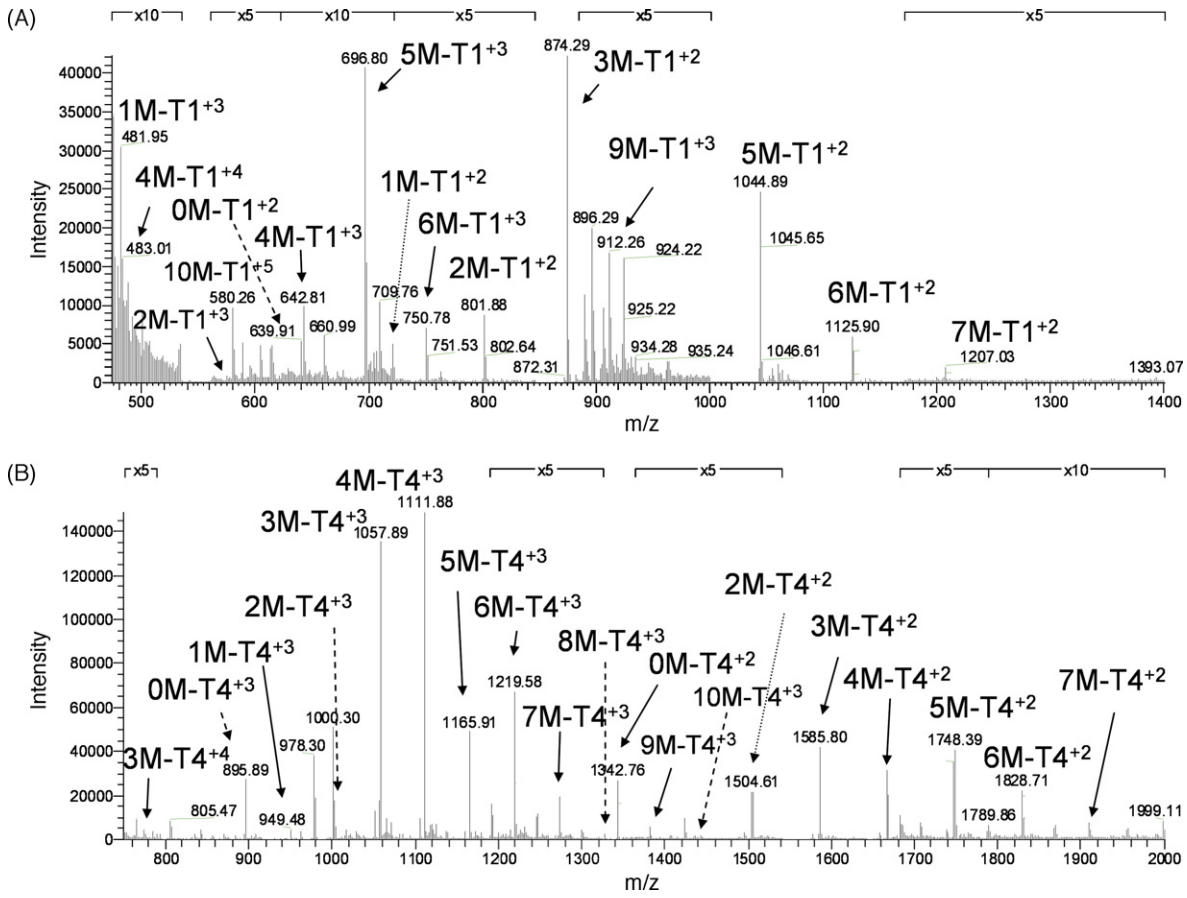

Fig. 5. LC/MS Full scan mass spectra of tryptic glycopeptide mixture showing the multiple charge states of (A) T1 and (B) T4 glycopeptides containing variations 1–10 mannosylations.

using an alkaline β-elimination reaction [47], labeled with 2-AB, followed by NPLC/MS. NPLC/MS analysis was chosen over MALDI-TOF-MS for several reasons. First, it provides rapid oligosaccharide analysis. Smaller amounts of sample are required because the analysis can be performed in a single run instead of the multiple runs necessary to first collect fractions from the NPLC column and concentrate for MALDI analysis. Small oligosaccharides tend to be problematic for MALDI analysis due to interferences from matrix peaks making it a poor choice for analysis of these types of species [54]. Instead we chose a direct route by coupling traditional NPLC to ESI mass spectrometry. However, to do so we needed to optimize the NPLC method so that it was compatible with electrospray mass spectrometry. First, we needed to decrease the amount of ammonium formate from 250 mM to 50 mM that is traditionally used in this type of analysis to make it compatible with ESI [55]. To increase signal intensity of the 2-AB labeled glycans, sodium acetate was added to the mobile phase. Without additional sodium in the mobile phase, the mass spec signal was split between both proton and sodium peaks. Therefore, glycans were ionized with sodium to increase sensitivity. As shown in Fig. 4, six main fluorescent peaks and several smaller peaks from Tf-exendin were observed by NPLC. The molecular weight (MW) of each glycan was observed as the sodiated 2-AB labeled glycan (1 mannose *m*/*z* 323, 2 mannoses *m*/*z* 485, 3 mannoses *m*/*z* 647, 4 mannoses *m*/*z* 809, 5 mannoses *m*/*z* 971, and 6 mannoses *m*/*z* 1133). The largest glycan released from Tf-exendin contained six mannose sugars. As shown in Fig. 4, trimannose and tetramannose glycans each resolved into two peaks by NP chromatography (same MW) due to hydrogen bonding differences in the molecules. These represent differentially linked glycans containing the same number of sugar moieties. In other words, peaks 3 and 3b are trimannose isomers and 4 are 4b tetramannose isomers characteristic of a yeast glycosylation pattern [2]. The first mannose residue added is derived from dolichol phosphate-linked mannose during protein biosynthesis. Additional O-linked glycosylations in yeast are added as $\alpha 1 \rightarrow 2$ linkages for the second and third mannoses added and remaining mannoses are added as $\alpha 1 \rightarrow 3$ O-glycosidic linkages. Dimannose, trimannose, and tetramannose were the most abundant glycans found on the Tf-exendin protein. The relative abundance of each glycan is shown above the peaks in Fig. 4. Also shown in Fig. 4 are the relative abundances observed by NPLC/MS for hTf. Human Tf contains only 26% of the amount of glycan modification than Tf-exendin confirming that simply decreased content of mannose compared to Tf-exendin does not explain the greater hydrophilic elution behavior of native Tf during RP-HPLC (result not shown).

The protein was digested with trypsin to examine the glycopeptides. Tryptic peptides were separated by RP-HPLC coupled to an ESI linear ion trap mass spectrometer. T1 and T4 were observed to be the predominate glycopeptides. As shown in Fig. 5, this group of peptides were mannosylated from 1 to 10 times per peptide (various sites with glycan lengths ranging from 1 to 6 mannose moieties) making it an extremely heterogeneous composition. The full scan mass spectrum of various T1 glycopeptides showing their multiple charge states is displayed in Fig. 5A while B shows the full scan mass spectrum of the multiple charge states of the T4 glycopeptides. Concanavilin A was later used as a sample preparation step and again the T1 and T4 peptides were the predominant glycopeptides (data not shown).

The next method was developed to identify peptide sequence, glycosylation sites, and number of sugars at each amino acid by

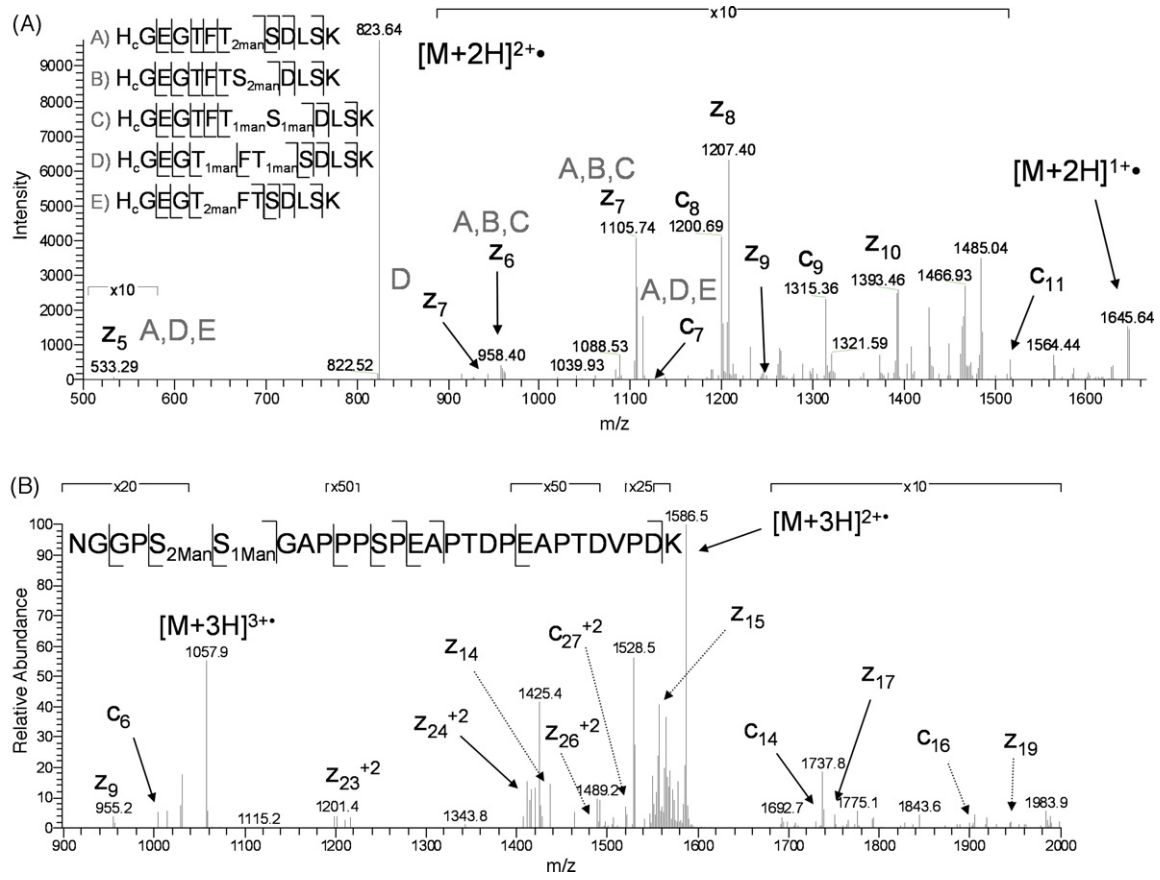

Fig. 6. ETD MS/MS spectra of mannosylated tryptic peptides. (A) MS/MS of *m*/*z* 823 mass spectra consistent with five variations of carbamylated T1 (H_{carb}GEGTFTSDLSK) tryptic peptide containing two mannose residues. (B) MS/MS of *m*/*z* 1058 consistent with +3 charge state of T4 trimannosylated tryptic peptide NGGP$S_{2man}S_{1man}$GAPPPSPEAPTDPEAPTDVPDK.

LC–tandem mass spectrometry using ESI-LIT. Neutral loss of mannose (162 Da) via CID was used to trigger subsequent ETD on the precursor ion. ETD MS/MS spectra were interpreted using BioWorks software and by hand to localize the glycans to their respective amino acids. This NL-dependent ETD method was developed and optimized to identify O-linked glycosylation sites in Tf-exendin peptides.

The N-terminal tryptic peptide, T1, has four O-linked sites (HGEGTFTSDLSK) and up to 10 mannoses were observed on this peptide in the full scan mass spectrum. The NPLC/MS glycan data showed that the largest intact glycan would be hexamannose. As a result, the longest possible mannose chain length attached to a single amino acid residue was therefore established to be six residues. In addition, all four O-linked sites were observed to be mannosylated. Fig. 6A shows the MS/MS ETD spectra of five T1-H_1 carbamylated dimannosylated peptides, mannosylated at various sites with either mono- or dimannose carbohydrate structures attached to the four possible glycosylation sites. The five peptides are labeled A–E and the *z* and *c* ions are labeled with the appropriate A–E label if the ion is specific to that peptide. If no A–E label is provided, the *z*/*c* ion pertains to all five structures. Some of the isobaric (same *m*/*z*) glycopeptides were resolved chromatographically which provided MS/MS spectra that were easier to interpret but these particular spectra were interesting in that all five glycopeptides can be distinguished in the same MS/MS spectrum. Most of the ETD spectra on the T1 peptides were +2 charge state ions due to the small size of the peptide which is not ideal for ETD. However, the spectra were often rich enough to determine the sequence and site of glycosylation. T4 was a larger peptide with higher charge states, but as explained below, was not the most ideal peptide either. Many hyper-mannosylated T1 peptides were observed and are listed in Table 1. We were able to verify the sites of glycosylation in the peptides containing 2–5 mannose sugars. In addition, a small percentage of the N-terminal histidine had been reported to be endogenously carbamylated (data not shown) [44].

Similar to the T1 results, T4 peptides were also mannosylated between 1 and 10 times as is displayed in Fig. 5B. T4 from Tf-exendin contains five glycosylation sites: three serines and two threonines. The T4 peptide sequence is difficult to resolve chromatographically due to the nine proline residues, each of which have cis–trans isomerization that is partially captured on the column resulting in a broad peak [56]. As the numbers of mannose groups increase the ionization efficiency of the peptide is likely to decrease [57]. These two factors combined make it a difficult peptide to capture for MS/MS experiments. The heterogeneity in the number of sugars (1–10), number of charge states observed, and the broadness of the peak combined to make structural assignments difficult. As mentioned, one benefit of the T4 peptide was that it ionized at a higher charge state to afford putative ETD structural determinations for this glycopeptide. The NL-dependent ETD method was able to isolate the +3 charge state of several T4 peptides. Data consistent with T4 glycopeptides sequences are shown in Table 1. The ETD MS/MS of *m*/*z* 1058 trimannosylated T4 peptide is shown Fig. 6B. In the spectra shown, the first serine is modified by a dimannose moiety and the adjacent residue, also a serine, is monomannosylated. While BioWorks provided a scored list of many peptides, the peptides confirmed by hand are listed in Table 1. If only partial ETD data was available in the spectra, the peptide was left out of the table. The full scan mass spectra provided additional data on the number of mannoses per peptide. CID spectra may also contain orthogonal

Table 1
Examples of glycopeptides consistent with MS/MS (ETD) data. T1 and T4 glycopeptides were modified with up to 10 mannose sugars at various sites up to six at a single amino acid.

No. of mannoses	Peptide sequence with mannose sites
T1 peptides (0–10 mannoses/peptide)	
2	HEGEGTFT$_{2man}$SDLSK
2	HEGETFTS$_{2man}$DLSK
2	HEGEGTFT$_{1man}$S$_{1man}$DLSK
2	HEGET$_{1man}$FT$_{1man}$SDLSK
2	H$_{carb}$GEGTFT$_{2man}$SDLSK
2	H$_{carb}$GEGTFTS$_{2man}$DLSK
2	H$_{carb}$GEGTFT$_{1man}$S$_{1man}$DLSK
2	H$_{carb}$GEGT$_{1man}$FT$_{1man}$ SDLSK
2	H$_{carb}$GEGT$_{2man}$FTSDLSK
2	HEGEGTFT$_{2man}$SDLSK
2	HEGEGTFTS$_{2man}$DLSK
3	HEGEGTFTS$_{3man}$DLSK
3	HEGEGTFT$_{1man}$S$_{2man}$DLSK
3	HEGEGTFT$_{2man}$S$_{1man}$DLSK
3	HEGEGTFTS$_{2man}$DLS$_{1man}$K
3	HEGEGTFT$_{3man}$SDLSK
3	HEGEGT$_{1man}$FT$_{2man}$SDLSK
4	HGEGTFT$_{2man}$S$_{2man}$DLSK
4	HGEGT$_{2man}$FT$_{2man}$SDLSK
4	HGEGT$_{4man}$FTSDLSK
4	HGEGT$_{2man}$FT$_{1man}$S$_{1man}$DLSK
4	HGEGT$_{1man}$FT$_{1man}$S$_{2man}$DLSK
4	HGEGTFTS$_{4man}$DLSK
4	H$_{carb}$GEGTFT$_{2man}$S$_{2man}$DLSK
4	H$_{carb}$GEGTFT$_{3man}$S$_{1man}$DLSK
5	HGEGTFT$_{2man}$S$_{3man}$DLSK
5	HGEGTFT$_{3man}$S$_{2man}$DLSK
5	HGEGTFTS$_{5man}$DLSK
5	HGEGTFT$_{5man}$SDLSK
5	HGEGTFT$_{1man}$S$_{4man}$DLSK
5	HGEGTFT$_{4man}$S$_{1man}$DLSK
T4 peptides (0–10 mannoses/peptide)	
3	NGGP[SS]$_{3man}$GAPPPSPEAPTDPEAPTDVPDK
3	NGGPS$_{2man}$S$_{1man}$GAPPPSPEAPTDPEAPTDVPDK
4	NGGP[SS]$_{4man}$GAPPPSPEAPTDPEAPTDVPDK
5	NGGP[SS]$_{5man}$GAPPPSPEAPTDPEAPTDVPDK
5	NGGPSSGAPPPSPEAPTDPEAPT$_{5man}$DVPDK

information on the sequence of the peptide (not the glycosylation site). Optimization of the ETD method is in progress to confirm the identity of the other glycopeptides.

The compiled data in Table 1 show that there appear to be 5 preferred serine/threonine sites for mannosylation of Tf-exendin within the first 55 amino acids of the N-terminal sequence as shown in Fig. 3. These are the first two threonines and first serine on T1, and the first serine and second threonine on T4. Each of these sites contains the longest mannose chain lengths measured, but also several shorter versions of mannose chains are found. It is unclear if this pattern is due simply to conformational constrictions during oligosaccharide synthesis or if special functions such as glycoprotein compartmentalization or transport are linked with a specific mannose arrangement. Further structural characterization is ongoing.

Finally, adapting the current Butyl-HP HIC system to a larger scale operation involved increasing protein loading for optimal productivity. At 10.0 mg/mL protein load, the column approached an overloaded condition observed by a rapid increase in UV signal after the second wash (results not shown). This situation could possibly result in catastrophic protein breakthrough, particularly if the environmental temperature is not well controlled. Though an upper performance temperature limit was not established, operation of the column below 18 °C resulted in significant degradation of column performance and breakthrough during column loading. The practical upper protein loading limit was therefore established at 10.0 mg/mL resin at 18 °C. The results at 10.0 mg/mL protein loading for product purity and yields for subsequent runs at 400 mL Butyl-HP HIC column bed volume averaged 80.6% parent RP purity and 67.8% product yield ($n = 3$). Upon pilot scale operation of this step at a 20 L column bed volume and 10 mg/mL protein loading, product purity by RP was 80% parent purity and yield was 66% polished product. In conclusion, we have successfully developed and scaled up 5000-fold a robust HIC method for the separation of mannosylated glyocoforms (% main peak parent purity went from 52.5% in the load to approximately 80% purity by urea RP-HPLC in the pool) that is suitable for preparative purposes.

4. Conclusions

We have developed conditions for HIC suitable for commercial use using sodium sulfate salt to separate closely related neutral mannosylated variants of a recombinant yeast transferrin-exendin-4 fusion protein. Binding to the hydrophobic resin was dominated by the N-terminal exendin-4 and linker sequences but the glycoform variants of the protein resolved on the basis of overall carbohydrate content. Although the protein contains many putative O-linked sites for sugar addition, mannosylation was observed only on tryptic peptides T1 and T4 which were located within the first 55 amino acids of the N-terminus. NPLC/MS analysis of released glycans confirmed that the oligosaccharides were between 1 and 6 mannose residues in length. Tryptic mapping using NL-dependent ETD analysis supported our hypothesis that the N-terminus of the protein was hyper-mannosylated, specifically on T1 and T4, and that these glycopeptides were very heterogeneous. The NL-dependent ETD method was a powerful tool to both simplify the identification process in a heterogeneous mixture and identify the oligosaccharide sites. Future experiments include investigating the linkages via permethylation and tandem mass spectrometry. This work introduces new technological capabilities for the purification and characterization of glycosylated variants of relevant glycoproteins.

Acknowledgements

The authors would like to thank Robert Shell for chromatography scale-up and tech transfer, Ned Mozier, Meg Reusch, Mike Schlittler for helpful discussions on the project, James Carroll for mass spectrometry advice, Jason Starkey for glycan advice, Scott Allen for urea RP-HPLC method development, Kirk Keith for Con A and various other work.

References

[1] W. Melander, C. Horvath, Arch. Biochem. Biophys. 183 (1977) 200.
[2] S. Strahl-Bolsinger, M. Gentzsch, W. Tanner, Biochim. Biophys. Acta 1426 (1999) 297.
[3] G. Sofer, L. Hagel (Eds.), Handbook of Process Chromatography: A Guide to Optimization, Scale-up and Validation, Academic Press, San Diego, 1998, p. 387.
[4] A. Mahn, M.E. Lienqueo, J.A. Asenjo, J. Chromatogr. B 849 (2007) 236.
[5] H.P. Jennissen, Int. J. Bio-Chromatogr. 5 (2000) 131.
[6] B.C.S. To, A.M. Lenhoff, J. Chromatogr. A 1141 (2007) 191.
[7] J.L. Fausnaugh, L.A. Kennedy, F.E. Regnier, J. Chromatogr. 317 (1984) 141.
[8] T. Arakawa, L.O. Narhi, Biotechnol. Appl. Biochem. 13 (1991) 151.
[9] S.N. Timasheff, H. Inoue, Biochemistry 7 (1968) 2501.
[10] F.Y. Lin, W.Y. Chen, M.T.W. Hearn, Anal. Chem. 73 (2001) 3875.
[11] E. Haimer, A. Tscheliessnig, R. Hahn, A. Jungbauer, J. Chromatogr. A 1139 (2007) 84.
[12] T.W. Perkins, D.S. Mak, T.W. Root, E.N. Lightfoot, J. Chromatogr. A 766 (1997) 1.
[13] T.T. Jones, E.J. Fernandez, Biotechnol. Bioeng. 87 (2004) 388.
[14] A. Jungbauer, C. Machold, R. Hahn, J. Chromatogr. A 1079 (2005) 221.
[15] J.R. Swartz, Curr. Opin. Biotechnol. 12 (2001) 195.
[16] L. Barnes, A.J. Dickson, Curr. Opin. Biotechnol. 17 (2006) 381.
[17] C.A.S. Barnes, A. Lim, Mass Spectrom. Rev. 26 (2007) 370.
[18] G. Bogosian, B.N. Violand, E.J. Dorward-King, W.E. Workman, P.E. Jung, J.F. Kane, J. Biol. Chem. 264 (1989) 531.
[19] F. Baneyx, Curr. Opin. Biotechnol. 10 (1999) 411.

[20] M. Eng, V. Ling, J.A. Briggs, K. Souza, E. Canova-Davis, M.F. Powell, L.R.D. Young, Anal. Chem. 69 (1997) 4184.
[21] I.H.Y. Yuk, D.I.C. Wang, Biotechnol. Appl. Biochem. 36 (2002) 133.
[22] T.R. Gemmill, R.B. Trimble, Biochem. Biophys. Acta 1426 (1999) 227.
[23] R.V. Cordoba-Rodriguez, BioPharm Int. 21 (2008) 44.
[24] H.A. van Veen, M.E. Geerts, P.H. van Berkel, J.H. Nuijens, Eur. J. Biochem. 271 (2004) 678.
[25] L. Valmu, N. Kalkinnen, A. Husa, P.D. Rye, Biochemistry 44 (2005) 16007.
[26] S.V. Kaveri, S. Lacroix-Desmzes, J. Bayry, S. Dasgupta, A. Chtourou, in: WPO (Ed.), France, 2007.
[27] P.L. Storring, Trends Biotechnol. 10 (1992) 427.
[28] S. Hermeling, D.J.A. Crommelin, H. Schellekens, W. Jiskoot, Pharm. Res. 21 (2004) 897.
[29] I. Mukovozov, T. Sabljic, G. Hortelano, F.A. Ofosu, Thromb. Haemost. 99 (2008) 874.
[30] M. Imperiali, C. Thoma, E. Pavoni, A. Brancaccio, N. Callewaert, O. Oxenius, J. Virol. 79 (2005) 14297.
[31] L.C. Wasley, G. Timony, P. Murtha, J. Stoudemire, A.J. Dorner, J. Caro, M. Krieger, R.J. Kaufman, Blood 77 (1991) 2624.
[32] A. Varki, in: A. Varki, R. Cummings, J. Esko, H. Freeze, G. Hart, J. Marth (Eds.), Essentials of Glycobiology, Cold Spring Harbor Laboratory Press, Cold Spring Harbor, NY, 1999, p. 57.
[33] G. Walsh, Nat. Biotechnol. 24 (2006) 769.
[34] S. Pichuantes, A.T. Nguyen, A. Franzusoff, in: J.L. Cleland, C.S. Craik (Eds.), Protein Engineering: Principles and Practice, John Wiley & Sons, New York, 1996, p. 129.
[35] M.C. Bewley, B.M. Tam, J. Grewal, S. He, S. Shewry, M.E. Murphy, A.B. Mason, R.C. Woodworth, E.N. Baker, R.T.A. MacGillivray, Biochemistry 38 (1999) 2535.
[36] H. Zhang, X.-J. Li, D.-J. Wang, J. Chen, Y.-L. Li, M.-S. Shen, H.-Q. Fang, H.-P. Chen, Chin. J. Biotechnol. 21 (2005) 804.
[37] L.M. Steinlein, T.N. Graf, R.A. Ikeda, Protein Expr. Purif. 6 (1995) 619.
[38] P.J. Sargent, S. Farnaud, R. Cammack, H.M.P. Zoller, R.W. Evans, Biometals 19 (2006) 513.
[39] M. Lommel, S. Strahl, Glycobiology 19 (2009) 816.
[40] J.J. Coon, Anal. Chem. 81 (2009) 3208.
[41] H. Steen, M. Mann, Nat. Rev. Mol. Cell Biol. 5 (2004) 699.
[42] J. Wiesner, T. Premsler, A. Sickmann, Proteomics 8 (2008) 4466.
[43] J.E.P. Syka, J.J. Coon, M.J. Schroeder, J. Shabanawitz, D.F. Hunt, Proc. Natl. Acad. Sci. U.S.A. 101 (2004) 9528.
[44] M. Zolodz, R. Dufield, J. Carroll, N. Mozier, CA Separation Sciences Society Mass Spectrometry, Napa, CA, 2008.
[45] M.E. Doyle, J.M. Egan, Pharmacol. Ther. 113 (2007) 546.
[46] A.N. Krutchinsky, I.V. Chernushevich, V.L. Spicer, W. Ens, K.G. Standing, J. Am. Soc. Mass Spectrom. 9 (1998) 569.
[47] Y. Huang, Y. Mechref, M.V. Novotny, Anal. Chem. 73 (2001) 6063.
[48] J.T. Herberg, E. Raleigh, D.M. Boyle, 6th HIC-RP Bioseparation Conference, Napa, CA, 2009.
[49] G.R. Bousfield, V.Y. Butnev, J.-M. Bidart, D. Dalpathado, J. Irungu, H. Desaire, Biochemistry 47 (2008) 1708.
[50] T. Arndt, J. Kropf, Clin. Chem. 48 (2002) 2072.
[51] M.B. De la Calle Guntinas, G. Bordin, A.R. Rodriguez, Anal. Bioanal. Chem. 378 (2004) 383.
[52] S. Olah, T. Kremmer, M. Boldizsar, J. Chromatogr. B: Biomed. Sci. Appl. 744 (2000) 73.
[53] A.B. Mason, P.J. Halbrooks, J.R. Larouche, S.K. Briggs, M.L. Moffett, J.E. Ramsey, S.A. Connolly, V.C. Smith, R.T.A. MacGillivray, Protein Expr. Purif. 36 (2004) 318.
[54] F. Fenaille, M. Le Mignon, C. Groseil, L. Siret, N. Bihoreau, Rapid Commun. Mass Spectrom. 21 (2007) 812.
[55] G.R. Guile, P.M. Rudd, D.R. Wing, S.B. Prime, R.A. Dwek, Anal. Biochem. 240 (1996) 210.
[56] J.C. Gesquiere, E. Diesis, M.T. Cung, A. Tartar, J. Chromatogr. 478 (1989) 121.
[57] N.B. Cech, C.G. Enke, Mass Spectrom. Rev. 20 (2001) 362.